

Robustness of a vortex ring interacting with an axial rod

Swarandeeep Sahoo, Prafulla Sohoni and Debopam Das
Department of Aerospace Engineering
Indian Institute of Technology Kanpur
Kanpur, India

Abstract—Vortex rings are ubiquitous in nature as well in man-made devices such as starting jets and synthetic jets. Recently, useful applications of such flow structures in industry have been proposed that involve motion of vortex rings over an axially placed rod. Although free vortex rings are quite stable and propagate for long distances without disintegrating, the scenario is modified to a great extent in presence of such an interacting body. Thus, in the present study, we study their properties and robustness of vortex rings produced from an orifice, with an axial rod aligned symmetrically with respect to its direction of propagation. We find the effect of such vortex body interaction, with the help of flow visualizations, which reveals the extent of their sustainability under the given conditions.

Keywords—Vortex Rings, axial interaction, cylindrical rod

I. Introduction

Vortices and their dynamics have been the focus of fundamental research owing to their implementation in the study of unsteady flows. The dynamics of isolated rectilinear vortices have been explored to a great extent in the context of tornadoes and hurricanes. Yet, researchers in vortex dynamics have recently augmented their focus towards application of ring vortices. The utility of these fluid structures in pollution transport from chimneys (Shariff & Leonard (1992)) to extinguish fires at gas and oil wells (Akhmetov *et al.* (1980b)) have been the motivation for numerous theoretical and experimental work in this regard.

Vortex ring is a toroidal fluid mass, spinning around a circular loop. Once generated it propagates with a self induced velocity until it breaks down due to instability. These can easily be generated by impulsively moving a slug of fluid through a sharp edged orifice or a nozzle. Besides study of isolated vortex ring, investigations have been carried out to understand the instability mechanisms of flows induced by such fluid structures when they interact with solid boundaries.

On the other hand, for industrial applications, Lucey, Jr *et al.* (2003) have developed effective ways to use vortex rings. Having a concentric rod placed along the axis of propagation of the vortex ring, they utilize the region of maximum velocity and hence momentum for applications such as removal of surface deposits on a tube and also, as a heat exchanger where heat is transferred from a heated tubular plate to the vortex ring that carries it to a heat sink.

The efficiency of the purpose in such devices depends on the extent to which vortex rings generated in a like manner are able to propagate in the presence of the axial rod. In the

present study we address the effectiveness of such methods from the view point of stability of such flows. To this effect, an experimental investigation of flow of a vortex ring over an axial rod, is carried out in order to study the effect of the rod on the flow field of an otherwise isolated vortex ring.

II. Experimental Setup

The experimental apparatus used for generating vortex rings is shown in Fig. (1). It consists of a large tank of square cross section fixed to a heavy wooden base. The tank measures 0.5 m by 0.5 m and is 2m long. It is divided into two compartments by a square plate (0.5 m by 0.5 m) of 12mm thick. The plate is placed at a distance of 0.5 m from one end. The compartment of 0.5 m length is used as the "driving section" with a flat rectangular piston attached to one of its ends. The other compartment is used as the "test section" for observing the evolution of the vortex rings. This arrangement facilitates in leaving all electronic equipment outside the testing region in order to prevent undesired air motion produced by them.

The piston is attached to and driven by a loudspeaker (100 W) which sets into motion a slug of air volume through an orifice of diameter 75mm. The piston is made of a thick polystyrene sheet which almost fits the walls of the chamber. The gaps are sealed using a flexible polythene strips, the edges of which are attached on one side to the edges of the piston while the other to the glass tank walls. This allows a smooth and unobstructed motion of the piston against the walls without rubbing on its surface, at the same time, ensuring a leak proof arrangement.

The loudspeaker is driven by a forcing signal that is first synthesized and stored in the non-volatile memory of an arbitrary function generator. A TTL trigger signal from the NI-DAQ (NI USB 6210) card is used to trigger the signal generation which is then amplified by a power amplifier and fed to the speaker.

A trapezoidal signal with smooth corners is used to drive the speaker. The distance moved by the piston is denoted by "Stroke Length" (L_p) while the time taken for the piston to push the fluid is denoted by "Stroke Time" (T_p). The signal 'peak to peak' voltage range determines L_p while the rise time of the signal is T_p . The trajectory of the piston is tracked from images taken using a high speed camera operating at 100 Hz frame rate. A typical velocity variation of the piston, obtained by differentiating the experimentally measured trajectory, is shown in Fig. (2).

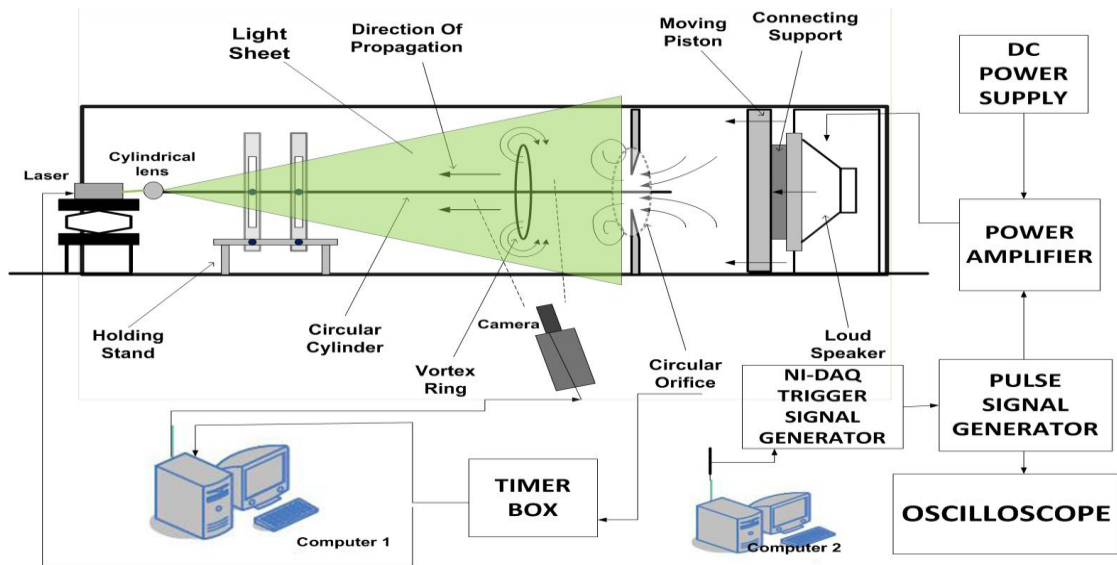


Figure 1. Schematic diagram of the experimental setup.

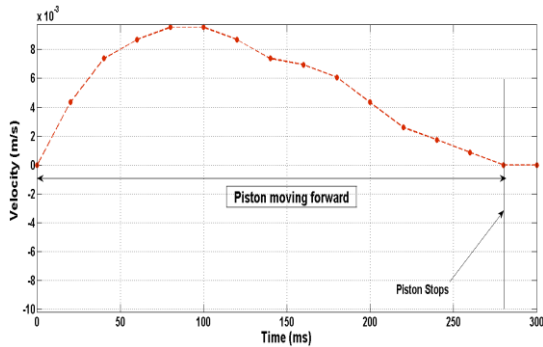


Figure 2. Variation of piston velocity with time.

The jet Reynolds number based on the diameter of the orifice D_o is defined as:

$$Re_{Jet} = \frac{U_M D_o}{\nu} \quad (1)$$

Where ν is the kinematic viscosity of air at 30°C (temperature at which the experiments are performed). (U_M) is the average ejection velocity defined as:

$$U_M = \frac{L_P}{T_P} * \frac{A_P}{A_O} \quad (2)$$

Where A_p is the area of the piston and $A_o = \frac{\pi}{4} D_o^2$, the exit area. In terms of piston motion quantities that are measured directly from the experiment, jet Reynolds number is obtained as:

$$Re_{Jet} = \frac{4 L_P A_P}{\pi T_P \nu D_o} \quad (3)$$

Experiments were carried out for the interacting vortex ring using a cylindrical glass rod of 4 mm diameter, held by a stand. The rod is aligned with the center of the orifice exit. The cylinder is placed such that it is 150mm ($\approx 2D_o$) distance

inside the orifice. Thus, the flow starts interacting with the rod as soon as the fluid is ejected from the annular hole thus formed. The complete set-up for flow visualization experiments is also depicted in Fig. (1).

A continuous laser (1.2 W) and a high speed camera of resolution 1028*1296 pixels is used to visualize the flow seeded with smoke particles. The laser sheet, created using a cylindrical lens is made to lie in a vertical plane passing through the rod's axis. Due to refraction from the edges of the rod, the light sheet had lines of shadow region developed onto it. In order to tackle this problem either we have taken image for one half of the ring or sometimes we forsake capturing areas close to the rod surface.

III. Observations

The evolution of the flow is observed from the point of start of piston motion. A range of Reynolds number was chosen, according to the definition given by Eqn. (3), for studying the effect for various cases. Under isolated condition, i.e., vortex ring formed without the presence of the rod, the evolution of the diameter and velocity were found to be similar as observed by earlier researchers. After the initial roll-up, the vortex ring propagates with almost constant velocity until for fairly long distance. Then it starts to become wavy and breaks down eventually.

For the condition with the rod inside the orifice, the exit configuration is effectively a circular annular hole. As soon as the piston motion starts, the fluid coming out of the annular region is confronted with two solid boundaries. One is the sharp periphery of the orifice, while the other is a long cylindrical surface of the rod in the central region.

As soon as the piston starts moving, a slug of fluid is pushed from annular exit. At this point, it is remarkable to note that the presence of the two surfaces present extreme cases of boundary geometry for the flow. The sharp orifice

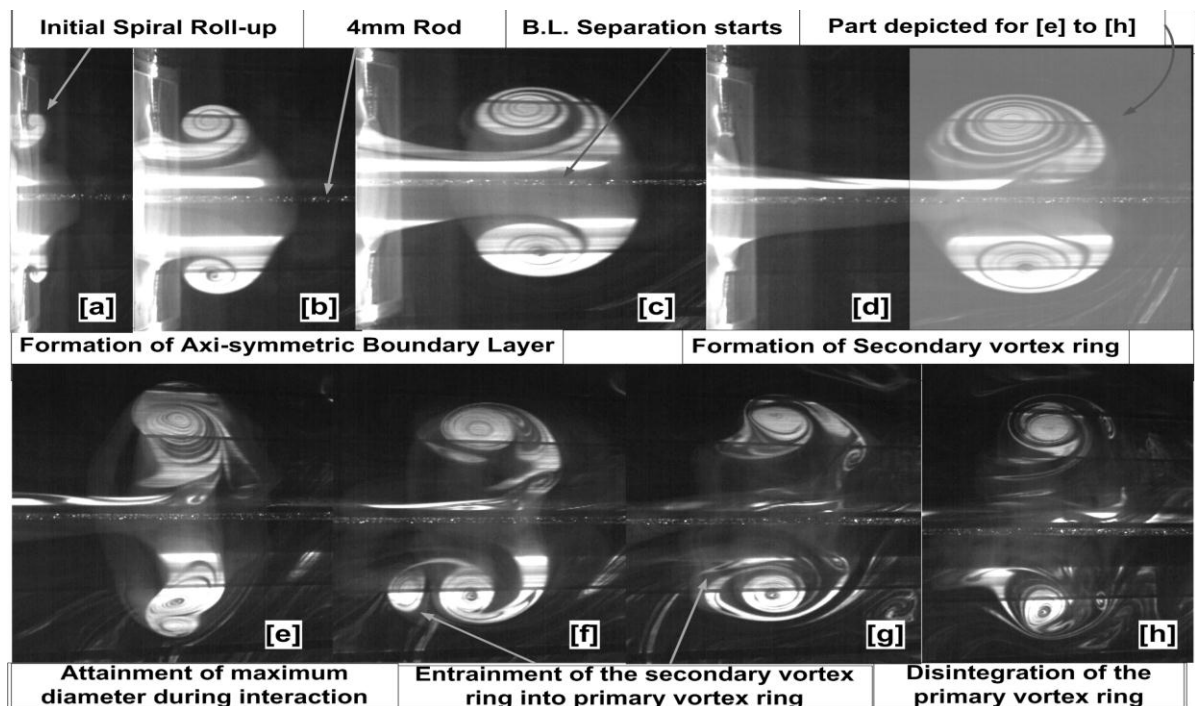


Figure 3. Flow visualization images depicting the evolution of a vortex ring and its interaction as it moves over the rod.

edge forces the flow to turn around by 180° while the rod surface creates no such tendency.

The flow immediately separates at the orifice edge and evolves in a manner similar to the roll-up of an isolated vortex ring. Meanwhile, the flow region near the rod develops an unsteady boundary layer on the surface. This boundary layer gradually becomes thicker due to gradual momentum loss experienced by the flow due to the wall shear stress. Eventually, the flow separates after some time due to the adverse pressure gradient region created by the very structure of the flow induced by the primary vortex ring.

The separated flow rolls up into a secondary vortex ring, which is of opposite strength to that of the primary ring (see Fig. (3) [e] to [h]). On account of the completion of the formation of the primary vortex ring and its self induced propagation, the separated flow region is also drifted in the axial direction, unlike the case uniform flow over a flat plate in adverse pressure gradient, where the separated bubble is stationary. This happens until, the relative strengths of both the secondary and primary ring are comparable and their mutual interaction mechanism comes into play.

The flow dynamics due to mutual interaction of both the vortex rings was also observed. The secondary vortex ring is convected around the periphery of the primary ring due to induction effect of the latter on the former. Eventually, the secondary vortex is entrained into the primary one which then moves ahead. A part of the primary ring fluid is lost into the wake during merging of the two rings.

Meanwhile, the forward axial flow is re-established near the rod surface. This near wall flow again forms a boundary layer which later forms a separated vortex like the previous

observation. Even though the pattern repeats up to three times in some cases, the intermittent interactions heavily distort the flow structure of the primary vortex ring. Repeated loss of vortical fluid, due to interaction of two opposite circulation vortex rings, into the wake greatly reduces the strength and thus facilitates rapid disintegration of the primary ring.

iv. Results and Analysis

Characteristics of the vortex rings during formation and propagation is obtained by measuring the diameter (D) and velocity of propagation (V_{vr}) during their evolution. The diameter of vortex ring and its propagation velocity variation with distance from the annular exit, (x), is shown in Figs. (4) and (5). The conditions for the vortex ring with and without the presence of the rod are depicted by unfilled and filled circles respectively. The diameter (D) and axial distance, (x), has been non-dimensionalized by the orifice diameter (D_0).

Note that the vortex ring diameter is similar for both conditions to a great extent during the formation phase. The boundary layer separation induces a radial velocity due to which the diameter is increased. The rise in diameter continues upto the point where the secondary vortex ring is at the top of the primary vortex ring.

Remarkably the velocity of the vortex ring increases in the presence of the rod. This can be explained from the fact that the flow now has a relatively lesser area to move, as the diameter is almost same, and thus speeds up axially. However, the increase in diameter of the primary vortex ring during interaction with the secondary vortex ring results in an interval of rapid decrease and subsequent regain of the self-induced velocity.

Table 1. Experimental Results

| Case | L_P (mm) | T_P (ms) | Re_{jet} | D/D_0 (WOR) | D/D_0 (WR) | V (WOR) (m/s) | V (WR) (m/s) | x_{sep} | T_{sep} |
|------|------------|------------|------------|---------------|--------------|-----------------|----------------|-----------|-----------|
| 1 | 83.5 | 285 | 1401 | 1.08 | 1.05 | 0.15 | 0.16 | 80.6 | 620 |
| 2 | 105.8 | 305 | 1659 | 1.13 | 1.11 | 0.23 | 0.25 | 87.3 | 410 |
| 3 | 150.3 | 330 | 2179 | 1.15 | 1.17 | 0.27 | 0.35 | 95.6 | 350 |
| 4 | 194.8 | 360 | 2588 | 1.18 | 1.27 | 0.37 | 0.46 | 111.7 | 310 |
| 5 | 217.1 | 370 | 2807 | 1.21 | 1.32 | 0.41 | 0.48 | 117.6 | 300 |
| 6 | 244.9 | 380 | 3083 | 1.21 | 1.35 | 0.48 | 0.57 | 133.4 | 292 |

WOR: Without rod WR: With rod

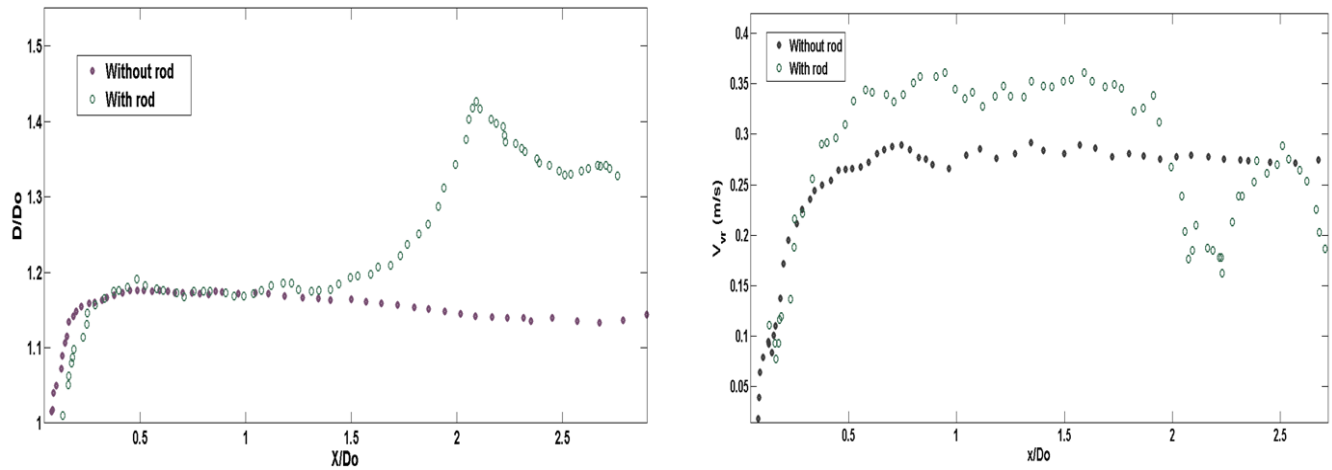


Figure 4. [a]:Normalised diameter and [b]: translation speed of vortex rings with and without the presence of cylinder for Case 3.

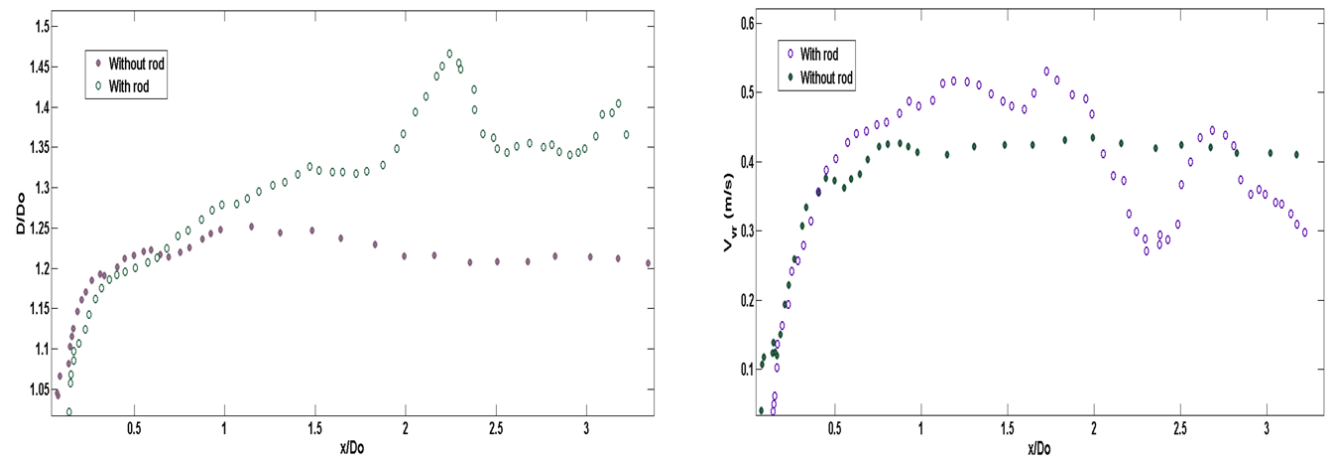


Figure 5. [a]:Normalised diameter and [b]: translation speed of vortex rings with and without the presence of cylinder for Case 4.

The experimental results are listed in Table. (1). The cases described for various stroke time and stroke length of the piston provides us with Reynolds number ranging from 1400 to 3100. The axial distance up to which the vortex ring travels in presence of the rod, without any boundary layer separation, is denoted by x_{sep} while the corresponding time is T_{sep} .

It is observed that for higher Reynolds number, vortex rings travel longer distances without succumbing to the effect of the rod. On the other hand, the time of their undisturbed existence gets reduced for the above variation in Re_{jet} .

The values for non-dimensional vortex ring diameter, D/D_0 , and its velocity of propagation V_{vr} , given in the table, are measured at the location $x/D_0 \approx 1.5$, the approximate distance at which the formation process of the vortex ring is complete. We also, hereby, note that, the diameter of the vortex ring ceases to remain similar for both conditions at higher Reynolds number. Yet, the effect of acceleration in axial direction is consistently more prominent with increase in the Reynolds number over the entire range.

v. Conclusions

The present investigation was carried out in order to assess the robustness of vortex rings moving over axially placed rods that are symmetrically aligned. The flow visualizations provide the nature of the flow evolution for two very different conditions of fluid and solid body interactions. Formation of the vortex ring and its propagation is affected due to a simultaneous development of boundary layer flow. The

interaction of the separated vortex with the primary ring determines the extent of the sustainability of the latter.

For the purpose of heat transfer applications, vortex rings of higher Reynolds number would be more suitable, as it is important to have larger region of the rod to enhance the heat exchange. On the other hand, for particle transport applications, it would be more appropriate to employ vortex rings of lower Reynolds number. The entrainment effects are more pronounced if we have longer duration of sustainability, achieved under such conditions.

References

- [1] K Shariff, and A Leonard, "Vortex Rings." Annual Review of Fluid Mechanics, 1992 Vol. 24: 235-279.
- [2] D.G. Akhmetov, B.A. Lugovtsov, V.F. Tarasov, "Extinguishing gas and oil well fires by means of vortex rings." Fiz. Goreniya Vzryva, 1980b Vol. 5: 8-14.
- [3] G. K. Lucey Jr., T. Gher, G. Cooper, R. J. Richter, "Methods for using a ring vortex." United States Patent, 2003, US006544347B2.,